PHYSICAL REVIEW A **75**, 041401(R) (2007)

Effects of molecular symmetry on enhanced ionization by intense laser pulses

G. Lagmago Kamta[1,2] and A. D. Bandrauk[1]
[1]*Département de Chimie, Université de Sherbrooke, Sherbrooke, Québec, Canada J1K 2R1*
[2]*Department of Medical Physics, McGill University, Montréal, Québec, Canada H3G 1A4*
(Received 28 October 2006; published 2 April 2007)

When molecules are driven by intense laser fields linearly polarized along the internuclear axis, their ionization rate vs the internuclear separation R is known to have a maximum at some critical intermediate separation R_c. We show that such a maximum should occur only in molecules whose highest occupied molecular orbitals (HOMOs) are such that the electron cloud is concentrated along the internuclear axis (i.e., σ-type HOMOs). For molecular systems whose HOMO symmetry prevents electron probability distribution along this axis, we find that the ionization rate increases monotonically with increasing R until saturation occurs. In other words, for such molecular systems, there is no critical R_c at which molecular ionization is maximum.

DOI: 10.1103/PhysRevA.75.041401 PACS number(s): 33.80.Rv, 33.80.Eh, 42.50.Hz, 33.80.Wz

As molecular systems stretch beyond their equilibrium internuclear separation, the ionization rate is enhanced, reaching a peak rate at some critical internuclear separation R_c. The peak rate is orders of magnitude larger than the rate at either small or large internuclear separation [1,2]. This effect is known as charge resonant enhanced ionization (CREI) and occurs when the polarization of the external laser field is parallel to the internuclear axis. EI has been predicted by theoretical studies [1–7], and confirmed by experiments [8–12]. Although initially predicted for one-electron diatomic molecules, the occurrence of a critical R_c for maximum EI appears to be a quite universal phenomenon, since experiments have found its signature not only in multielectron diatomic molecules [8–10], but also in more complex molecules such as CO_2 [13]. In addition, theoretical calculations also suggest the occurrence of EI in atomic clusters [14,15].

Theoretical investigations of EI have been done using one-dimensional (1D) molecular models [2,4], as well as realistic 3D approaches for H_2^+ [1,5,6], HeH^{2+} [7]. On the other hand, experiments have used Cl_2 [8], I_2 [9], I_2^+ [10], H_2^+ [11,12], and D_2^+ [12] molecules as targets. These molecular systems have one common feature: the highest occupied molecular orbital (HOMO) or the initial state has a σ-type symmetry, i.e., the electron cloud in these HOMOs is concentrated along the nuclei. In this paper, we investigate EI in molecular systems whose electron cloud in the initial state is not concentrated along the internuclear axis. This is the case for molecules such as O_2 and F_2, which have π ground state orbitals. For such molecules and the ones commonly used in experiments, theoretical studies of their interaction with intense laser fields can only be done using gross approximations [16,17]. However, essential symmetry properties of most diatomic molecular orbitals can be reproduced by appropriately chosen orbitals of the simplest molecule H_2^+, for which the 3D time-dependent Schrödinger equation (TDSE) can be solved numerically. This means that insight into symmetry-related effects involving HOMOs of complex molecules can be gained by studying their symmetry analog for H_2^+ [18]. In this perspective we solve the 3D TDSE for H_2^+ driven by intense laser pulses linearly polarized along the internuclear axis, using initial states (i.e., active orbitals) having various symmetries. It is found that for active orbitals having π and δ symmetries the ionization probability increases quasimonotonically with increasing internuclear distances, thereby suggesting that there is no critical R_c at which EI is maximum. We show that this is due to the fact that electrons in these orbitals are kept off the nuclei by symmetry forces, so that electrons actually experience a Coulomb potential that is almost atomiclike.

The electronic motion of H_2^+ is described by the TDSE $i\frac{\partial}{\partial t}\Psi(\mathbf{r},t)=[\mathbf{p}^2/2+V(\mathbf{r})+\mathbf{A}\cdot\mathbf{p}]\Psi(\mathbf{r},t)$, where $\mathbf{p}=-i\nabla$ is the electron momentum, $V(\mathbf{r})=-1/|\mathbf{r}+\mathbf{R}/2|-1/|\mathbf{r}-\mathbf{R}/2|$ is the Coulomb attraction of the electron due to the nuclei. $\mathbf{r}\equiv\mathbf{r}(x,y,z)$ is the electron distance relative to the center of mass of the molecule, where (x,y,z) are the Cartesian coordinates. We make the dipole approximation, and assume that the nuclei are fixed along the z axis with internuclear distance R, i.e., $\mathbf{R}=R\mathbf{e}_z$, where $\mathbf{e}_z$ is the unit vector along the z axis. $\mathbf{A}(t)=f(t)A_0\sin(\omega t)\mathbf{e}_z$ is the vector potential of the laser pulse linearly polarized along the z axis. A_0, $f(t)$, and ω, respectively, denote the maximum amplitude, the envelop, and the frequency of the laser pulse. In this paper, we use a cosine-squared laser pulse and its total pulse duration τ is given in units of the laser period $T=2\pi/\omega$. Unless stated otherwise, atomic units (a.u.) are used.

The TDSE is solved in spheroidal coordinates (ξ,η,ϕ) using the following expansion of $\Psi(\mathbf{r},t)$:

$$\Psi^m(\xi,\eta,\phi,t)=\sum_{\mu\nu}a^m_{\mu\nu}(t)U^m_\nu(\xi)V^m_\mu(\eta)\frac{e^{im\phi}}{\sqrt{2\pi}}, \qquad (1)$$

where $\xi=(r_1+r_2)/R$, $\eta=(r_1-r_2)/R$, and ϕ is the azimuthal angle. m is electron's angular momentum projection along the z axis. $a^m_{\mu\nu}(t)$ are time-dependent coefficients, and the basis functions $U^m_\nu(\xi)$ and $V^m_\mu(\eta)$ involve Laguerre and Legendre polynomials, respectively. For more details on the basis expansion see Refs. [20–22]. The TDSE is solved using a semi-implicit Rosenbrock method [7,19]. This *ab initio* approach yields stationary eigenvalues and eigenvectors of H_2^+, as well as their ionization probability and harmonic spectra with high accuracy [7,18,20–22]. Since the laser is linearly polarized along the z axis, the dipole operator does not couple states having different m values, i.e., m is conserved throughout the time propagation of the TDSE. This

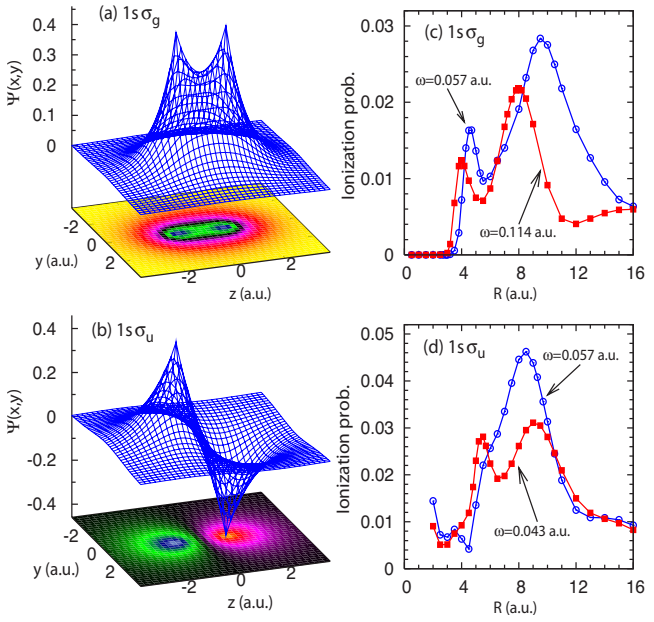

FIG. 1. (Color online) Left plots show the wave function $\Psi(y,z)$ and the corresponding contour plot for the following eigenstates of H_2^+ for $R=2$ a.u.: (a) $1s\sigma_g$; (b) $1s\sigma_u$. Right plots show the ionization probability vs R obtained using the initial state shown on the left plot. The laser pulses used have the peak intensity 10^{14} W/cm^2, the frequency ω shown and a total time duration $\tau=3T$. Dots represent the calculated data, and lines are shown to guide the eye.

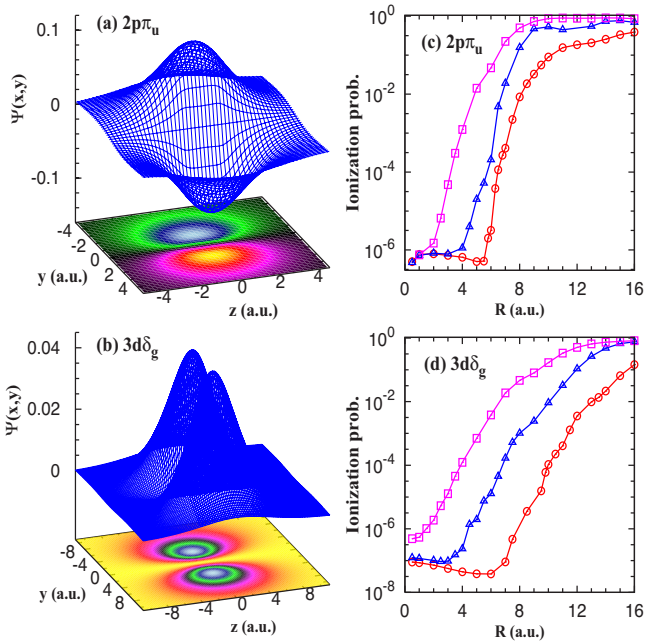

FIG. 2. (Color online) $\Psi(y,z)$ as in Fig. 1 for the following eigenstates of H_2^+ for $R=2$ a.u.: (a) $2p\pi_u$; (b) $3d\delta_g$. Right plots illustrate the R- and intensity dependence of the ionization probability obtained using the initial state shown on the left: (c) $2p\pi_u$ initial state, $\omega=0.02$ a.u., $\tau=3T$, for peak intensities $I=10^{13}$ W/cm^2 (squares), $I=4\times10^{12}$ W/cm^2 (triangles), $I=2\times10^{12}$ W/cm^2 (circles); (d) $3d\delta_g$ initial state, $\omega=0.01$ a.u., $\tau=3T$, for $I=10^{12}$ W/cm^2 (squares), $I=5\times10^{11}$ W/cm^2 (triangles), $I=10^{11}$ W/cm^2 (circles).

justifies the label m in the wave function (1).

Figure 1 shows the wave functions $\Psi(y,z)\equiv\Psi(x=0,y,z)$ of $1s\sigma_g$ and $1s\sigma_u$ states ($m=0$) of H_2^+ vs the electron Cartesian coordinates (x,y,z), as well as the R dependance of the ionization probability obtained using each of these states as the initial state for propagating the TDSE. As Fig. 1 shows, the electron cloud in both states is concentrated along the internuclear axis z, and the antibonding character of the $1s\sigma_u$ leads to a vanishing wave function along the axis perpendicular to the z axis through the origin. The initial state $1s\sigma_g$ is used for results in Fig. 1(c), with laser frequencies $\omega=0.057$ a.u. ($\lambda=800$ nm) and $\omega=0.114$ a.u. ($\lambda=400$ nm). Figure 1(d) shows similar results, but for the initial state $1s\sigma_u$, with laser frequencies $\omega=0.057$ a.u. and $\omega=0.043$ a.u. ($\lambda=1064$ nm). As expected [1–6], one sees that EI occurs for both $1s\sigma_g$ and $1s\sigma_u$ initial cases, as the ionization probability increases drastically when R reaches some intermediate value. In addition, there is a critical internuclear distance R_c at which EI is maximum. This critical distance, which depends on the laser intensity and frequency, is $R_c\approx10$ a.u. and $R_c\approx8$ for the respective frequencies $\omega=0.057$ a.u. and $\omega=0.114$ a.u. when the initial state is $1s\sigma_g$. For the $1s\sigma_u$ initial state, $R_c\approx9$ a.u. and $R_c\approx8$ for $\omega=0.043$ a.u. and $\omega=0.057$ a.u., respectively. In addition, the antibonding character of $1s\sigma_u$ and the fact that this state is not the lowest level of H_2^+ are irrelevant to the occurrence of EI and the existence of R_c for maximum EI.

The electronic wave functions for $2p\pi_u$ ($m=1$) and $3d\delta_g$ ($m=2$) are illustrated in Figs. 2(a) and 2(b). The ionization probability obtained using these as initial states is shown in Figs. 2(c) and 2(d), respectively. These figures indicate that for small R's the ionization probability depends only slightly on R. But as R increases to reach some intermediate value, the ionization probability increases drastically and keeps increasing as the molecule stretches further, until saturation occurs, so that there is no critical R_c for which EI is maximum. This is in stark contrast with the case of σ initial states in Fig. 1 where there exist a R_c beyond which stretching the molecule decreases the ionization rate.

The $2p\pi_u$ and $3d\delta_g$ orbitals share a common feature that distinguishes them from σ orbitals in Figs. 1(a) and 1(b). This feature is the presence of a nodal axis along the internuclear axis z where the wave function vanishes. Note that we have recently showed the ionization rate is suppressed (compared to other molecular orientations) when the laser polarized along this axis [18], leading to an image of the molecular orbital. This nodal symmetry constraint forces the electron cloud to be concentrated away from the z axis. Even in a laser field linearly polarized along this z axis, electrons are still kept away from the internuclear axis. Indeed, Fig. 3 shows a snapshot of the electron probability distribution $|\Psi_c(y,z)|^2$ at the end of the laser pulse for initial states $1s\sigma_g$ and $2p\pi_u$. All bound states have been removed from the final wave function $\Psi_c(y,z)$, which therefore describes the ionized electron. It appears that for the $1s\sigma_g$ initial state in Fig. 3(a), the electron is concentrated along the internuclear axis; this feature is observed for all σ states. In contrast, for the $2p\pi_u$ state in Fig. 3(b), the electron cloud is kept off the

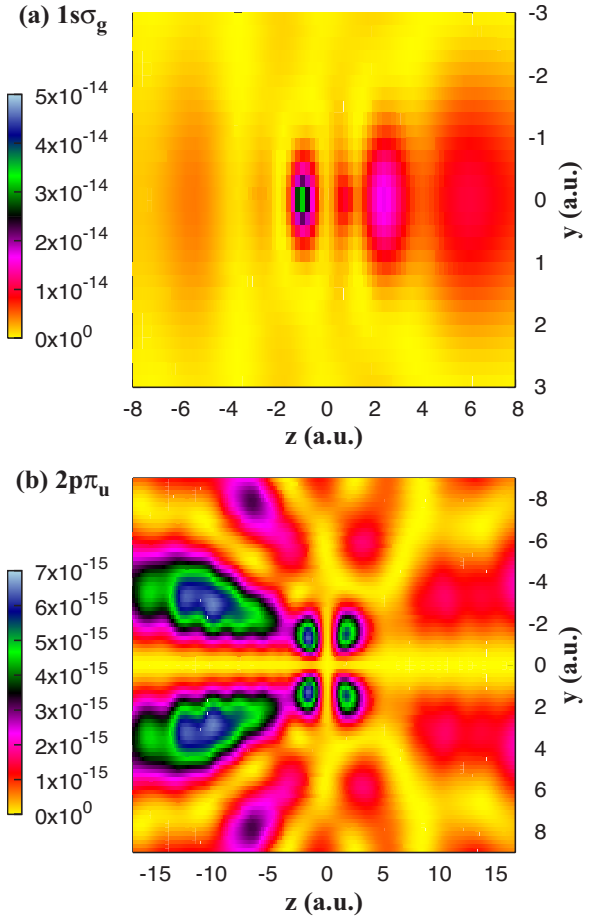

FIG. 3. (Color online) Snapshots of the probability distribution $|\Psi_c(y,z)|^2$ of the ionized electron at the end of the laser for the states $1s\sigma_g$ and $2p\pi_u$. Laser parameters are $\omega=0.057$ a.u., $I=10^{14}$ W/cm^2, and $\tau=3T$ for (a), and $\omega=0.02$ a.u., $I=10^{13}$ W/cm^2, and $\tau=5T$ for (b).

nuclei, and concentrated along an axis parallel to the internuclear axis near $y\approx 2$. This is also the case for the $3d\delta_g$ initial state, and more generally for any wave function for which $m\neq 0$. This can be shown by considering the fact that any function $\Psi(\mathbf{r},t)$ of an arbitrary vector $\mathbf{r}(r,\theta,\phi)$ in spherical coordinates can be expanded in a series of spherical harmonics $Y_\ell^m(\theta,\phi)$ as [23]: $\Psi(\mathbf{r},t)=\Sigma_{\ell,m}\psi_{\ell m}(r,t)Y_\ell^m(\theta,\phi)$. Since the z axis corresponds to having $\theta=0$ and since $Y_\ell^m(\theta=0,\phi)=0$ for any $m\neq 0$ [see, e.g., Eqs. (5.2.2) of Ref. [23]], then $\Psi^m(r,\theta=0,\phi,t)=0$ for $m\neq 0$. In other words, all electronic wave functions for which $m\neq 0$ vanish along the quantization axis z. Similarly, one can show using bipolar spherical harmonics that this property also holds for systems with two active electrons in L-S coupling.

It follows that throughout the laser excitation electrons in σ states are concentrated along the internuclear axis z, while those in other states ($m\neq 0$) remain off the internuclear axis. In order to understand how this situation is responsible for the difference in EI in Figs. 1 and 2, we plot in Fig. 4 the combined potential $W(y,z)\equiv V(x=0,y,z)+Fz$ experienced by the electron in a static field F for various R's. For fixed y, $W(y,z)$ gives a 1D illustration of the effective potential experienced by an electron along the z axis at a distance y from

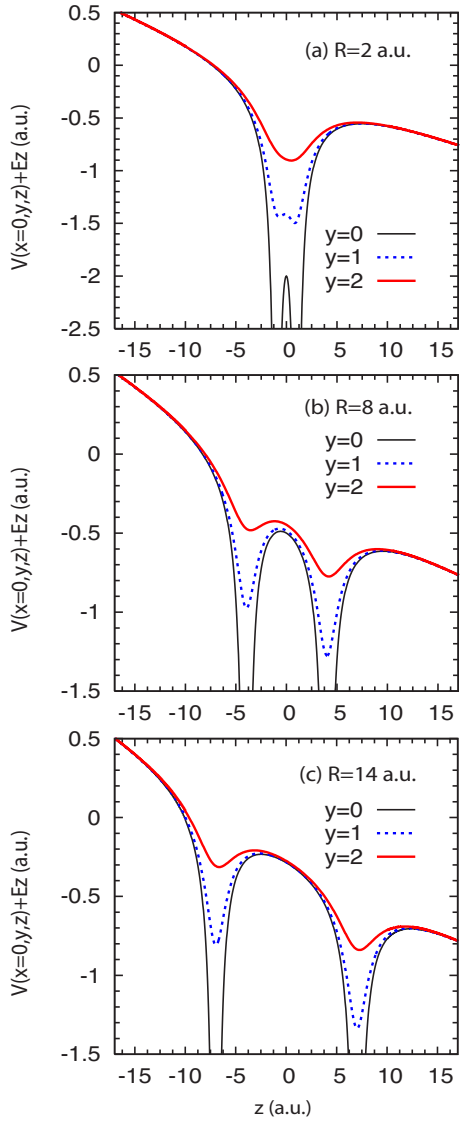

FIG. 4. (Color online) Combined Coulomb and static field potentials $W(y,z)=V(x=0,y,z)+Fz$ for (a) $R=2$ a.u.; (b) $R=8$ a.u.; (c) $R=14$ a.u. In each case, $W(y,z)$ is plotted for $y=0$ a.u. (dark solid lines at bottom), $y=1$ a.u. (dashed lines), $y=0$ a.u. (red solid lines at top). In all cases, $F=0.038$ a.u. (i.e., $I=5\times 10^{13}$ W/cm^2).

this axis. Each plot in Fig. 4 shows $W(y,z)$ for $y=0$ a.u., $y=1$ a.u., and $y=2$ a.u. Therefore, σ states concentrated along the z axis see the effective potential $W(y=0,z)$, whereas π states whose electron cloud is concentrated parallel to the z axis at the distance $y\approx 2$ a.u. experience the effective potential $W(y=2,z)$.

Let us revisit the origin of R_c for σ states in the context of tunnel ionization [24], which is based on nonadiabatic localization [1–3,5] of the electron wave function in the rising well (i.e., left wells in Fig. 4). Electrons in σ states see the effective potential $W(y=0,z)$ represented by solid dark lines (SDL) in Fig. 4. At small R [see SDL in Fig. 4(a)], the inner barrier of the double well potential is so low that electrons in σ states do not fully experience the double well nature of the potential. In this case, the rate of ionization is similar to that of the united atom. At some intermediate R [see SDL in Fig.

4(b)] near the critical R_c, the ionization is enhanced because the electron can tunnel across or fly above the narrow inner potential barrier into the continuum. As the molecule stretches further to a larger internuclear distances [see SDL in Fig. 4(c)] electrons are increasingly localized on one or the other well, due to the raising and widening inner barrier between the two wells. This hinders tunneling between the two wells, leading a decrease in the ionization at large R's, approaching the separated atom limit.

Electron clouds in molecular systems with $m \neq 0$ are localized at some distance $y \neq 0$ from the internuclear axis, and therefore do not experience the full strength (the singularity) of the Coulomb attraction, which is maximum near the nuclei. Therefore, as illustrated in Fig. 2, significant ionization of such molecules occurs at fairly low intensities. Electrons localized at $y \neq 0$ experience a quite different effective potential in the vicinity of the nuclei. As y increases in Fig. 4, one sees that while the effective potential at large z is unchanged, its depth near the nuclei rises quickly. At small R's [see dashed lines and red solid lines in Fig. 4(a)], the effective potential has a single well, and the ionization is atomiclike. With increasing R, the inner potential barrier rises and so does the minimum of the rising left potential well (this feature is absent in σ states). At some intermediate R, the rising minimum of the left potential becomes higher than the right potential barrier, leading to a strong enhancement of molecular ionization. Here, electrons can tunnel through the thin inner potential well directly into the continuum. In addition, any electron wave packet localized on the left potential well is also above the right potential well, which further boosts the ionization rate. In contrast to the σ states where the rising inner potential well hinders ionization, the raising minimum of the left well for $m \neq 0$ states prevents or minimizes electron localization on either well. Even at large R in this case, any electron wave packet (for bound or excited state) localized on the left well is automatically above the right potential well. Such a wave packet can easily tunnel through the inner potential barrier and fly above the right barrier directly in the continuum. In other words even at large R, tunnel ionization of electron wave packets from both wells remains strong, leading to a steady increase of ionization with increasing R, until saturation occurs. The mechanism discussed here (i.e., off-axis electron charge density and strong field driving along the laser polarization) can also explain the decreasing strength of EI with increasing angle between the molecular axis and the laser polarization, observed for σ states in Ref. [25].

Our *ab initio* calculations for H_2^+ in a laser pulse linearly polarized along the internuclear axis indicate that the orbital symmetry strongly influences enhanced ionization in molecules. Enhanced ionization for σ states is known to peak at a some internuclear distance. We find that this peak in the ionization rate can only occur for σ states. Indeed, for molecular systems with other orbital symmetry ($m \neq 0$), we have shown that enhanced ionization occurs, but with no critical R_c for maximum ionization, i.e., the ionization rate increases steadily until saturation. This is due to the fact that for molecular systems having nonzero angular momentum projection along the internuclear axis, the wave function vanishes along this axis, leading to a distortion of the effective potential experienced by orbital electrons. We expect this effect to occur also in more complex molecules such as O_2, whose HOMO also has a nodal axis along the internuclear axis.

[1] T. Zuo and A. D. Bandrauk, Phys. Rev. A **52**, R2511 (1995).
[2] T. Seideman, M. Y. Ivanov, and P. B. Corkum, Phys. Rev. Lett. **75**, 2819 (1995).
[3] K. Codling *et al.*, J. Phys. B **22**, L331 (1989); K. Codling and L. J. Frasinski, *ibid.* **26**, 783 (1993).
[4] S. Chelkowski and A. D. Bandrauk, J. Phys. B **28**, L723 (1995).
[5] Z. Mulyukov, M. Pont, and R. Shakeshaft, Phys. Rev. A **54**, 4299 (1996).
[6] I. Kawata, H. Kono, and Y. Fujimura, J. Chem. Phys. **110**, 11152 (1999).
[7] G. Lagmago Kamta and A. D. Bandrauk, Phys. Rev. Lett. **94**, 203003 (2005).
[8] M. Schmidt, D. Normand, and C. Cornaggia, Phys. Rev. A **50**, 5037 (1994).
[9] D. Normand and M. Schmidt, Phys. Rev. A **53**, R1958 (1996).
[10] E. Constant, H. Stapelfeldt, and P. B. Corkum, Phys. Rev. Lett. **76**, 4140 (1996).
[11] G. N. Gibson, M. Li, C. Guo, and J. Neira, Phys. Rev. Lett. **79**, 2022 (1997).
[12] D. Pavičić, A. Kiess, T. W. Hänsch, and H. Figger, Phys. Rev. Lett. **94**, 163002 (2005).
[13] A. Hishikawa, A. Iwamae, and K. Yamanouchi, Phys. Rev. Lett. **83**, 1127 (1999).
[14] V. Veniard, R. Taieb, and A. Maquet, Phys. Rev. A **65**, 013202 (2001).
[15] C. Siedschlag and J. M. Rost, Phys. Rev. Lett. **89**, 173401 (2002); Phys. Rev. A **67**, 013404 (2003).
[16] J. Muth-Böhm, A. Becker, and F. H. M. Faisal, Phys. Rev. Lett. **85**, 2280 (2000).
[17] X. M. Tong, Z. X. Zhao, and C. D. Lin, Phys. Rev. A **66**, 033402 (2002).
[18] G. Lagmago Kamta and A. D. Bandrauk, Phys. Rev. A **74**, 033415 (2006).
[19] W. H. Press *et al.*, *Numerical Recipes in Fortran: The Art of Scientific Computing*, 2nd ed. (Cambridge University Press, Cambridge, 1992).
[20] G. Lagmago Kamta and A. D. Bandrauk, Phys. Rev. A **70**, 011404(R) (2004).
[21] G. Lagmago Kamta and A. D. Bandrauk, Phys. Rev. A **71**, 053407 (2005).
[22] G. Lagmago Kamta and A. D. Bandrauk, Laser Phys. **15**, 502 (2005).
[23] D. A. Varshalovich, A. N. Moskalev, and V. K. Khersonskii, *Quantum Theory of Angular Momentum* (World Scientific, Singapore, 1988).
[24] With parameters used in this work, the Keldysh parameter is less than 1, indicating that we are indeed in the tunneling regime.
[25] T. K. Kjeldsen, L. B. Madsen, and J. P. Hansen, Phys. Rev. A **74**, 035402 (2006).